



Vancouver, Canada

June 13-16, 2018/ *Juin 13-16, 2018*

BLAST LOADS ON STRUCTURES

Elassaly Mohamed^{1,4}, Salem Mohamed^{2,5}, Mohsen Alaa.³

¹Prof. Of Structure, Faculty of Engineering, Fayoum University

²Lecturer of Reinforced concrete, Housing and Building National Research Center

³Graduate student, Structural Engineering Dept., Fayoum University, Fayoum, Egypt

⁴ mohamed.elassaly@gmail.com

⁵ mm.aladawy@gmail.com

Abstract: Over the last decades, using of explosives by terrorist groups around the world that target high occupancy and public buildings, has become a growing problem in the world. Explosive devices have become smaller in size and more powerful than some years ago, leading to structural failure or massive damage in buildings. It also could result in extensive life loss or serious injuries. Terrorists usually use vehicle bombs in order to increase the number of injuries and fatalities and cause extensive damages to properties. The present research presents a thoroughly documentation of the most significant terrorism events in Egypt that happened in government officials, police, tourists and religious buildings. In addition, the research examines the pressure time history that results from the explosions using the computer program Vector-Blast which is based on the blast wave characteristics of TNT scale. This would help in predicting future potential damages that could happen with different explosives types and quantities, for RC structures having various parameters.

1 INTRODUCTION

Most of the damaged structures by bombs or impact loading are not designed to resist blast loads. Many countries, all over the world, have experienced increase in terrorism events; thus, there is a great need to better understanding of the effects of explosives on structures. These effects include shock wave physics and pressure, besides thermochemistry of explosives. In order to understand a structure's resistance to explosives, pressure-time history must be predicted accurately at various points on the structure. When the atmosphere surrounding the explosion is pushed back, an external blast wave will be created due to a massive energy coming outside from the center of the explosion. The front of the wave has a pressure greater than the region behind it; then, it immediately begins to decay as the shock propagates outward. Explosives create an incident blast wave, characterized by instantaneous rise from atmospheric pressure to a peak overpressure. As the shock front expands, pressure decays back to ambient pressure, leading to a negative pressure phase, that occurs usually in longer duration than the positive phase as shown in Figure 1. The negative phase is usually less important in the design process than the positive phase. When the incident pressure wave, on a structure, is not parallel to the direction of the wave's travel path, it is reflected producing what is known as reflected pressure. The reflected pressure is always greater than the incident pressure, at the same distance from the explosion. The reflected pressure varies with the angle of incidence of the shock wave and the incident pressure, as shown in Figure 2. When the shock wave is perpendicular to the exposed surface, the point of impact will experience the maximum reflected pressure. When the reflecting surface is parallel to the blast wave, minimum reflected pressure will occur.

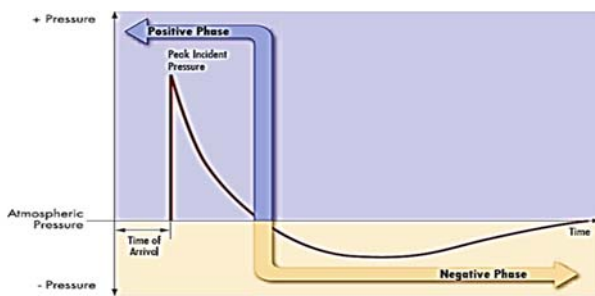


Figure 1: Blast pressure-time history (FEMA-426 2003)

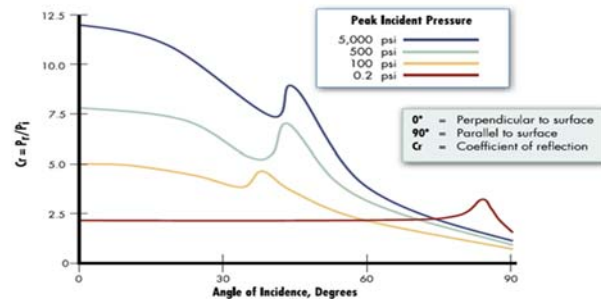
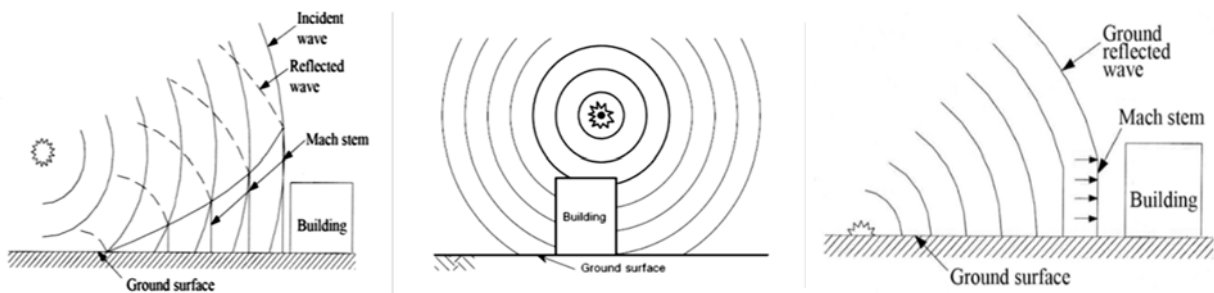


Figure 2: Reflected pressure coefficient vs. angle of incidence (FEMA-426 2003)

Explosions are classified into two major categories (TM 5-1300 1990): External and Internal. External explosions are outside blasts, in an open environment, while internal explosions occur inside a covered container or building. An external blast wave can be classified into air burst, free air burst and surface burst, depending on whether the point of detonation of the explosive is above, at or below the ground surface (Figure 3).



(a) Air burst with ground reflections

(b) Free-air burst explosion

(c) Surface burst

Figure 3: Classifications of external blast load (Jayasooriya 2010)

All blast parameters depend on the quantity of energy released by the explosion (or charge weight) and distance from the origin of the explosion to the building. This distance is called stand-off distance, as shown in Figure 4. The threat of the explosion will rapidly decrease over the stand-off distance. Scaled distance defined by cube root method can be calculated from the following equation:

$$[2] \text{ Scaled distance, } (z) \text{ in } \text{m/kg}^{1/3} = \frac{R}{W^{1/3}}$$

$$[1] R = \sqrt{(X_b - X_{AP})^2 + (Y_b - Y_{AP})^2 + (Z_b - Z_{AP})^2}$$

Where R is ray path distance (Figure 5), W is the mass of TNT charge equivalent

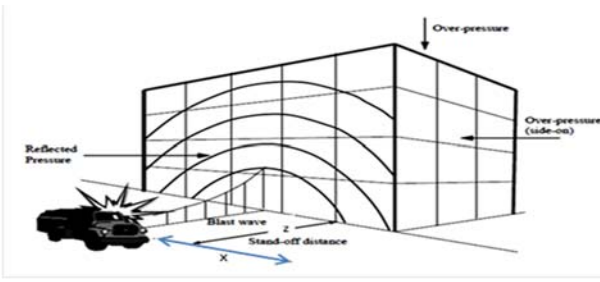


Figure 4: Stand-off distance (Moon 2009)

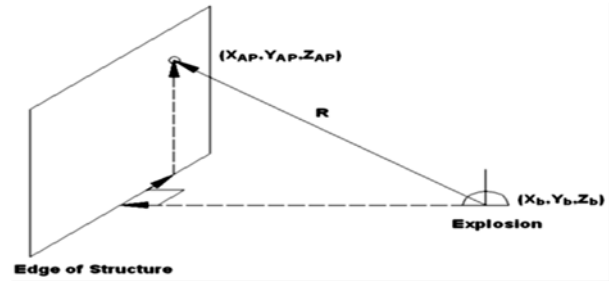


Figure 5: Simple ray path calculation (Miller 2004)

When a point on the wave front hits a corner, it diffracts around it. The process of diffraction causes energy to be sent into all directions. The pressure and impulse loading on the structure are greatly reduced as part of the energy from the incident wave ray is transferred to the structure.

Dharaneepathy et al. 1995, tested models of cylindrical structures, having heights of 100, 200, and 300 m and with 5m diameters. The charge weight was 125 kg of TNT, at distances varying from 30 to 110 m, using numerical simulations. The results indicated that there exists a critical ground zero distance at which the blast response reaches the maximum values; this distance should be used as the design datum distance. Ripley et al. 2004, examined the effects of wave reflection and diffraction angle on a structure. They used a charge mass of 50g of C4 having dimensions (2.5x2.5x5.0cm), located at three separate stand-off distances. Good numerical values of the pressure-time histories were recorded. The effect of diffraction angle was investigated. The results were considered acceptable, since the estimated pressure and impulse results were different by almost 19% and 15%, respectively from the experimental ones. For all charge locations, numerical results were found to be less than experimental values but were considered acceptable. They concluded that the Chinook code is able to capture the effects of diffraction, blast channeling and complex wave reflection, accurately. Kakogiannis et al. 2010, studied the blast wave numerically by two types of finite element methods: Eulerian multi-material modeling and pure Lagrangian using CONWEP (Hyde, 1992). They compared it with the experimental ones. In the first type of simulations, pressure waves were calculated by multi-material Eulerian formulation. For the Lagrangian finite element models, the load was applied as an equivalent triangular pulse. The Eulerian models provided results closer to the experimental ones. In general comparison with experimental, results showed that the combination of both versions CONWEP implementation and Eulerian multi material modeling were considered efficient design tools. Pranata and Madutujuh 2012, designed a blast resistant single door to bear 0.91 bar blast pressure and 44 ms blast duration. Dynamic elastic finite element method was carried out with 900 nodes using computer software ADINA. The dynamic time history analysis modeled blast load as Impact load for the given duration. The numerical analysis was done in order to know the behavior under blast load and estimate the safety margin of the door. Shallan et al. 2014, investigated the effects of blast loads on three buildings using the finite element program AUTODYN. They studied two story buildings with three different aspect ratios 0.5, 1.0 and 1.5; explosive load was equivalent to 1000 kg of TNT, placed at 2.0m height from the ground. They concluded that the reflected overpressure temperature of different points in the building increase with decrease of the standoff distance of the blast load from the building. The arrival time of reflected over pressure and temperature increase with increasing standoff distance. The blast load, at distance, equals 1.5m from the building, made a total failure in the column in the face of the blast load. Netherton and Stewart 2016, compared deterministic and probabilistic methods in blast loading. They noticed that deterministic blast loading methods did not fully account for society's usual acceptance (or rejection) of the risks associated with damage, safety and injury, as a result of an explosive blast-load. The authors concluded from the prediction of blast-loads using probabilistic models, three important forms of risk-advice: Risk Mitigation Advice, the Probability of Safety Hazards and the cost-benefit analysis of risk mitigation proposals.

In the present research work, some of the most important explosions in Egypt and other countries have been documented. An analysis program Vector-Blast (Miller 2004) is applied on those buildings. Vector-Blast is an analytical tool designed to calculate pressure-time histories at specified points on the front, rear faces and on the sides of the structure. Blast load characteristics and dissipation with time, are calculated.

Pressure time histories are calculated for different TNT charges and standoff distances, in order to predict peak reflected pressure for any building. The outcomes of this study should be used in the design of blast resistance building, with graphical interfaces.

2 EXPLOSIVES AND TNT EQUIVALENT

Explosives are different from one to another by their explosion characteristics such as detonation rate, effectiveness and amount of energy released. TNT is considered the datum for explosions “Explosion Bench Mark”. Explosives are often expressed in terms of standard TNT equivalent mass (R.E.) in the process of prediction, as presented in Table 1.

Table 1: Different equivalent TNT common explosives (https://en.wikipedia.org/wiki/TNT_equivalent)

No.	Explosive Type	Density (lbs./ft ³)	Detonation Vel.(ft/s)	R.E.
1	HMTD (hexamine peroxide)	54.8	14829.2	0.74
2	ANFO (94% AN + 6% fuel oil)	57.3	17289.8	0.74
3	Nitromethane (NM)	70.4	20865.9	1.10
4	ANNMAL (66% AN + 25% NM + 5% Al + 3% C + 1% TETA)	72.3	17585.1	0.87
5	Dynamite, Nobel's (75% NG + 23% diatomite)	92.2	23621.8	1.25
6	Amatol (50% TNT + 50% AN)	93.4	20636.2	0.91
7	Semtex 1A (76% PETN + 6% RDX)	96.6	25163.7	1.35
8	Amatol (80% TNT + 20% AN)	96.6	21554.9	1.10
9	Composition C-4 (91% RDX)	99.1	26377.6	1.34
10	Trinitrotoluene (TNT)	99.7	22637.5	1.00
11	Trinitrobenzene (TNB)	99.7	23949.8	1.20
12	Tetrytol (70% tetryl + 30% TNT)	99.7	24179.5	1.20
13	Gelignite (92% NG + 7% nitrocellulose)	99.7	26148.0	1.60
14	Composition C-3 (78% RDX)	99.7	25032.5	1.33
15	Composition A-5 (98% RDX + 2% stearic acid)	102.8	27788.4	1.60
16	Pentolite (56% PETN + 44% TNT)	103.4	24671.6	1.33
17	Tritonal (80% TNT + 20% aluminium)*	105.9	21817.3	1.05
18	Composition B (63% RDX + 36% TNT + 1% wax)	107.2	25721.5	1.33
19	Ammonium nitrate (AN + <0.5% H ₂ O)	107.2	8858.2	0.42
20	Hexogen (RDX)	110.9	28543.0	1.60
21	Torpex (aka HBX, 41% RDX + 40% TNT + 18% Al + 1% wax)	112.1	24409.2	1.30
22	PBXW-11 (96% HMX, 1% HyTemp, 3% DOA)	112.8	28608.6	1.60
23	Hexanitrobenzene (HNB)	122.7	30839.5	1.85
24	Mercury(II) fulminate	275.4	13943.4	0.51

3 EXAMINED CASE STUDIES

A sample of ten buildings are chosen as case studies for the application of program Vector-Blast. Those buildings were affected by bombs in different forms of destruction. The weights of bombs in those events ranged from 176 to 20062 lbs. of TNT equivalent. Table 2 presents a summary of properties of those buildings, date of events and dimensions of buildings. In addition, characteristics of explosives are presented, including ways or methods of implementing the explosives, equivalent TNT charge and stand-off distances. Finally, Table 2 presents brief descriptions of the resulting destructions for those buildings as well as the pertained number of fatalities and injuries. The associated damages that occurred to some of those buildings, are also depicted in Figures (6 to 12).

4 ANALYSIS RESULTS

The computer program Vector–Blast (Miller 2004) is applied on all the above case study events. Vector-Blast estimates the reflected, incident and negative side-on peak pressure, for the different case studies having varying scaled-off distances and charge weight. Table 3 presents a summary of sample study outcomes of case study 2, for hypothetical ascending stand-off and scaled distances. Case study 2 resembles EL-Khobar towers, Saudi Arabia (1996) having the largest charge weight among investigated cases. Figures [13 and 14] depict the variation of reflected and incident peak pressure with scaled distance, respectively, for case study 2.

Implementing Vector-Blast for other investigated case studies, results in similar behaviour and outcomes for the reflected, incident and negative side-on pressure. Table 4 presents a summary of outcomes of all investigated case studies, arranged ascending according to scaled distances of each event. Figure 15 depicts the reflected pressure for all investigated case studies, combined in a single graph.

Table 2: Summary of the examined case studies

No	Event	Date	Building (Dim, ft.)	Method	TNT (lbs.)	Standoff distance (ft.)	Structural damage	Other related damages	Fatalities and Injuries	Ref.
1	Alfred P. Murrah Federal Building Oklahoma, U. S.	19-4-1995	W= 239 D= 88.6 H= 131	Truck Bombing	3968	Z= 16.4 X= 141 Y= 0	Shear cracking of the floor slabs Two columns were buckled at third floor. Girder rotate inward. One third of the building damaged.	A hole (D=7.87, W=98.4 ft.). 324 buildings within a 4-block radius damaged 86 cars were burnt The glass was shattered in 258 nearby buildings. \$652 million of damage.	168 Fatalities, 680 Injuries	https://en.wikipedia.org/wiki/Oklahoma_City_bombing
2	Al Khobar towers Saudi Arabia	25-6-1996	W= 148 D= 39.4 H= 78.7	Truck bomb	20062	Z = 72 X= 65.6 Y = 0	Security fence windows and concrete building Windows were shattered up to (1.6 km) away	A hole (W=85, D=36 ft.) Felt in state of Bahrain; 32 km away Destruction of: Six high rise buildings Several military vehicles	19 Fatalities, 498 Injuries	https://en.wikipedia.org/wiki/Khobar_towers_bombing
3	Hilton Taba South Sinai Egypt	7-10-004	W= 243 D= 59 H= 118	Truck bomb	794	Z=2.79 X = 29.5 Y = 0	Ten floors of the hotel collapsed following the blast.		34 Fatalities, 171 Injuries	https://en.wikipedia.org/wiki/2004_Sinai_bombing
4	Islamabad Marriott Hotel Pakistan	20-9-2008	W= 410 D= 82 H= 98.4	Truck bomb	~ 28666	Z = 98.4 X = 220 Y = 0	A gas pipe blown up Fire engulfed The reception area	Crater (W=65.6, D=19.7 ft.) Windows in nearby buildings hundreds of yards away.	54 Fatalities, 266 Injuries	https://en.wikipedia.org/wiki/Islamabad_Marriott_Hotel_bombing
5	Saints, St. Mark & Pope, Peter I Alex. Egypt.	1-1-2011	W=197 D=115 H=32.8	Vehicle bomb	176	Z = 32.8 X = 82 Y = 0	Glass broke but remained in the window frame Doors stayed in frames but will not be reusable.	Two cars exploded next to the original car. Windows and doors broke in the opposite mosque.	21 Fatalities, 43 Injuries	https://www.christianheadlines.com/news/trauma-grips-survivors-of-church-blast-in-alexandria-egypt
6	South Sinai Security Directorate Egypt	7.10.2013	W=95 D=95 H=62	Car bomb	441	X= 82 Z= 46 Y = 0	Glazing broke and Shattered away. Doors were broken.	A 3.28 ft. depth crater Damages in: Façade of the General Sec. Directorate of Education. 3 schools damaged. 6 cars were burnt.	3 Fatalities, 63 Injuries	http://www.ahr.org.eg/NewsPrint/251330.aspx

7	Mansoura Security Directorate Egypt	24.12.2013	W=164 D=144 H=52.5	Van bomb	3307	Z = 13 X = 98.4 Y = 0	Collapse of: Side facade First floor completely Second and third floors, partially.	A crater (D=9.84, W=16.4 ft.) Partial collapse in Mansoura City Council, National Theater, United Bank and police dept. Destroying police cars	16 Fatalities, 150 Injuries	https://en.wiki.pedia.org/wiki/December_2013_Mansoura_bombing
8	Cairo Security Directorate Egypt	24.1.2014	W=262 D=82 H=72	Pick-up bomb	3858	Z = 49 X= 105 Y= 0	Destruction of: Seven floor building Some RC roofs Chairs, offices, computers and air conditioner Facade, windows and doors	A hole (D=11.5, W=32.8 ft.) Destruction of: Islamic museum's poss. Museum's decorations, facade The Book House building Cairo Appeal Prison Criminal Investigation D. 50 police cars	4 Fatalities, 76 Injuries	http://www.albawabhnews.com/354381
9	Police dept. EL-ARISH	12-4-2015	W=98.4 D=82 H=32.8	Pick-up B.	1102	Z=32.8 Y=0 X=26.3	Destruction of: The glass facades Offices in three floors. Office furniture	A hole (D=39.4, W=6.56 ft.) Destruction of façades of adjacent buildings. 7 vehicles were burnt.	7 Fatalities, 44 Injuries	https://www.cbsnews.com/news/italian-consulate-bombed-in-
10	Italian Council, Cairo Egypt	11-7-2015	W=279 D=32.8 H:32.8	Car Bomb	992	Z=19.7 Y=0 X=197	Destruction some of: Consulate offices Glass and concrete Doors and fence Entrance and surrounding wall	Some damages in: The October 6 th bridge. Visa office & Water pipe Journalists' Syndicate B. The Higher Judicial Dept. Egyptian Museum Façade	1 Fatality, 44 Injuries	https://www.cbsnews.com/news/italian-consulate-bombed-in-



Figure 6: Murrah Federal Building in Oklahoma City, 1995 (before and after attack)



Figure 7: Al Khobar tower, Saudi Arabia, 1996



Figure 8: Hilton Taba in south Sinai, Egypt, 2004



(a) Mansoura security directorate



(b) The National Theater



Figure 9: Destruction of Mansoura Security Directorate and National Theater in Egypt, 2013



(a) Cairo security directorate



(c) Islamic Museum

Figure 10: Destruction of Cairo Security Directorate and Islamic Museum in Egypt, 2014



Figure 11: Third Police Department of EL-ARISH in Egypt, 2015



Figure 12: Italian council in Egypt, 2015

Table 3: Reflected, incident, dynamic, negative side-on peak pressure for hypothetical ascending stand-off and scaled distances of case study 2 (Al Khobar towers, Saudi Arabia, 1996)

Charge Weight (lbs.)	Standoff Distance (ft.)	Scaled Distance (ft./lb ^{1/3})	Reflected Peak PR (psi)	Incident PR (psi)	Dynamic PR (psi)	Negative side on PR (psi)
20062	8.20	0.302063609	53511.7	4604	19224.8	14.935
20062	9.84	0.362476331	43006.5	3819.5	15331.8	14.935
20062	13.12	0.483301775	29157	2737.8	10154.6	14.9205
20062	16.40	0.604127218	20700.8	2059.2	7081.55	14.8915
20062	19.69	0.724952662	15203.1	1610.5	5149.15	14.8335
20062	22.97	0.845778106	11667.5	1297.9	3858.45	14.7755
20062	26.25	0.966603549	9264.4	1069.7	2952.24	14.6885
20062	29.53	1.087428993	7536.78	896.67	2314.21	14.6015
20062	32.81	1.208254437	6247.62	761.64	1868.51	14.4855
20062	39.37	1.449905324	4487.74	567.27	1272.64	14.1955
20062	49.21	1.812381655	2680.48	390.6	772.343	13.485
20062	59.06	2.174857986	1830.07	279.46	487.751	12.818
20062	72.18	2.658159761	1083.93	184.22	273.209	11.2955
20062	82.02	3.020636092	757.176	138.14	182.338	9.831
20062	98.43	3.62476331	434.217	89.871	98.948	7.1775
20062	114.83	4.228890529	267.656	62.176	55.9845	4.872
20062	131.23	4.833017747	176.668	45.458	33.379	3.7845
20062	147.64	5.437144965	125.904	34.786	20.9525	3.19
20062	164.04	6.041272184	92.771	27.579	13.7895	2.7695
20062	196.85	7.249526621	53.911	18.72	6.7425	2.2185
20062	229.66	8.457781057	36.337	13.659	3.683	1.885
20062	262.47	9.666035494	26.1	10.382	2.204	1.711
20062	328.08	12.08254437	16.0515	6.8585	1.0295	1.276
20062	393.70	14.49905324	11.136	4.959	0.5655	1.044
20062	459.32	16.91556211	8.2795	3.8425	0.348	0
20062	524.93	19.33207099	6.5685	3.132	0.232	0
20062	590.55	21.74857986	5.423	2.639	0.1595	0
20062	656.17	24.16508874	4.5965	2.2765	0	0
20062	787.40	28.99810648	3.5235	1.7545	0	0
20062	984.25	36.2476331	2.61	1.305	0	0
20062	1148.29	42.28890529	2.175	1.0875	0	0
20062	1354.99	49.900908024	1.8705	0.928	0	0

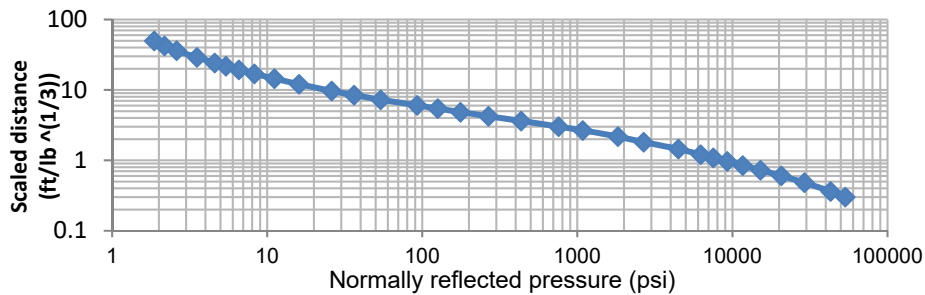


Figure 13: Variation of reflected peak pressure with hypothetical ascending scaled distance

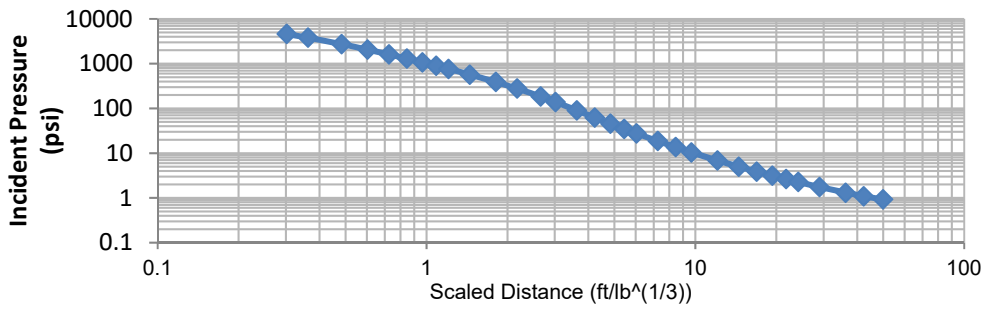


Figure 14: Variation of incident peak pressure with hypothetical ascending scaled distance

Table 4: Summary of outcomes, arranged ascending according to scaled distances of case study event

Case study No	Charge weight (lbs.)	Standoff Distance (ft.)	Scaled Distance (ft./lb ^{1/3})	Reflected Peak PR (psi)
3	794	2.79	0.3014	53644.9
7	3307	13.12	0.8815	10865.981
1	3968	16.40	1.0369	8196.89
10	992	19.69	1.9751	2265.886
2	20062	72.18	2.6582	1083.93
8	3858	49.21	3.1399	673.206
9	1102	32.81	3.1782	648.933
5	176	32.81	5.8543	102.6165
4	2866	98.43	6.9339	60.958
6	441	82.02	10.7837	20.4885

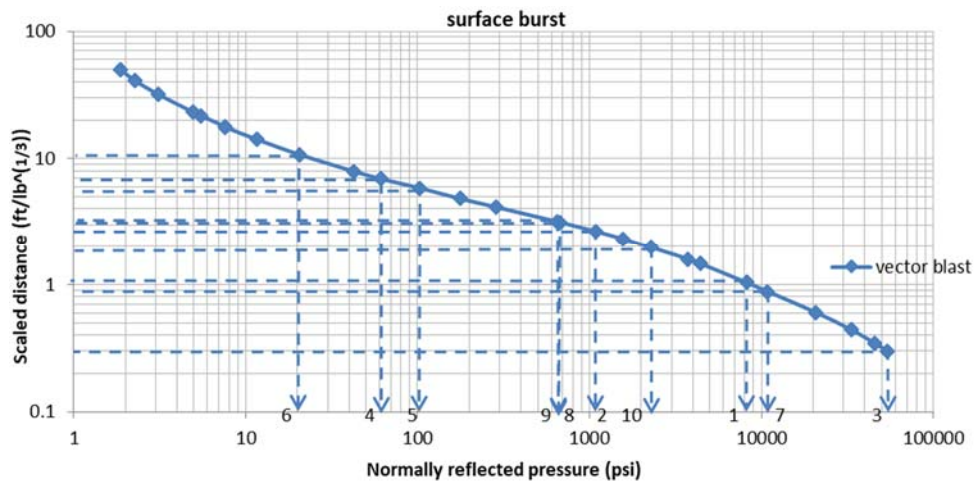










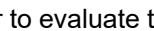
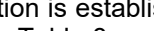
Figure 15: Scaled distance vs. normally reflected peak pressure

5 BLAST EFFECTS PREDICTIONS

The estimated capacity of TNT equivalent, pertained to the different ways, methods and vehicles used to deliver the weapon to the site of interest, is presented in Table 5. The expected level of damage in a building is estimated in Table 6, according to the incident pressure coefficient, C_r (FEMA-426 2003); C_r equals the

ratio of reflected to incident pressure. Accordingly, the level of damage of case study buildings, is predicted for the calculated pressure levels. Tables 7 summaries the predicted level of damage of case study building, which are conforming to the observed damage, during actual events.

Table 5: Capacity of TNT correlated with the way of explosive (Homeland Security Digital Library), <https://www.hsdl.org/?abstract&did=4506>

Diagram	Way of explosive	Capacity of TNT equivalent (lbs.)
	Pipe bomb	5
	Suicide bomber	20
	Brief case	50
	car	500
	suv	1000
	Small moving van	4000
	Delivery truck	4000
	Water truck	10000
	Large moving van	10000
	Semi-trailer	60000

Finally, in order to evaluate the range of likely charge weight that would lead to a specific damage mode or level, a correlation is established between the charge weight, mode of damage, and standoff distance for different cases. Table 8 and Figure 16 present this correlation, in which modes of damages are classified in to: Total destruction, column buckling, concrete wall failure, minor damage and finally glass breakage mode. Therefore, the expected damage mode in a building, could be estimated for a specific charge weight, way of explosive and standoff distance.

Table 6: Correlation of damage to Reflected Pressure Coefficient, Cr (FEMA-426 2003)

Damage	Reflected Pressure Coefficient, Cr=Pr/Pi
Typical window glass breakage	0.15 -0.22
Minor damage to some buildings	0.5 – 1.1
Panels of sheet metal buckled	1.1 – 1.8
Failure of concrete block walls	1.8 – 2.9
Collapse of wood framed buildings	Over 5
Serious damage to steel framed buildings	4 - 7
Severe damage to reinforced concrete framed buildings	6 - 9
Probable total destruction of most buildings	10 - 12

Table 7: Classification of level of damage of case study buildings according to reflected and incident pressures

Case study building	Level of Damage	Reflected peak Pressure, Pr (psi)	Incident Peak Pressure, Pi (psi)	Calculated Pressure coefficient, Cr _i	Typical range, Cr
Hilton Taba	Failure	53644.9	4613.639	11.63	10-12
Mansoura Directorate		10865.98	1334.29	8.14	
Murrah building	Severe	8196.89	963.67	8.5	6-9
Italian Council		2265.89	335.327	6.76	
Al-Khobar tower	Serious	1083.93	184.2225	5.88	
Cairo Directorate	to	673.206	126.266	5.33	>5
El-Arish police department	Severe	648.933	122.7425	5.29	
The Saints, St. Mark &	Serious	102.6165	29.5365	3.47	4-7

Peter I					
Islamabad Hotel	Partial	60.958	20.5465	2.97	1.8-2.9
South Sinai Directorate	Failure	20.489	8.4535	2.42	

Table 8: Blast damages rate correlated to charge weight

Charge weight	Threshold, total destruction	Threshold, column buckling	Concrete wall failure	Minor damage	Glass break
5	0.5130	1.7100	5.1299	10.2599	18.8097
20	0.8143	2.7144	8.1433	16.2865	29.8586
50	1.1052	3.6840	11.0521	22.1042	40.5243
100	1.3925	4.6416	13.9248	27.8495	51.0575
500	2.3811	7.9370	23.8110	47.6220	87.3071
1000	3.0000	10.0000	30.0000	60.0000	110.0000
4000	4.7622	15.8740	47.6220	95.2441	174.6141
10000	6.4633	21.5443	64.6330	129.2661	236.9878
60000	11.7446	39.1487	117.4460	234.8921	430.6354

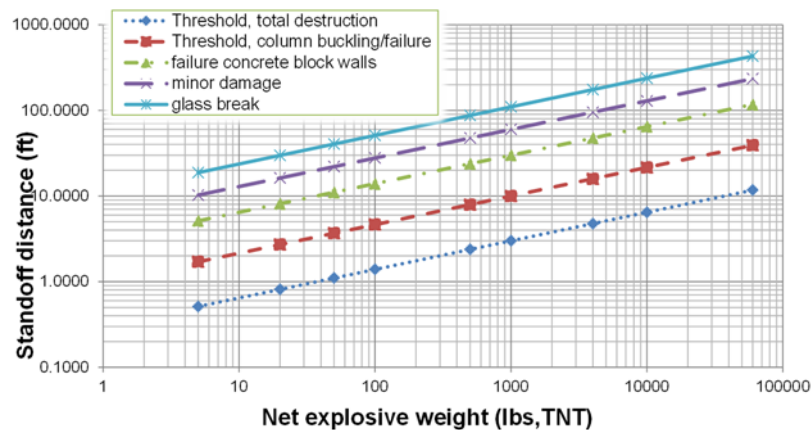


Figure 16: Blast range effects on reinforced concrete structures

6 CONCLUSIONS

The present study presents a documentation for the damage occurred to some events that occurred in Egypt lately, due to blast loads, resulting from different explosion scenarios. The damage level that occurred to 10 case study buildings, is investigated using Vector-blast analysis program. Blast loads varied between (176~20062 lbs.) of TNT charges and were located at different standoff distances (2.79~82 ft.). The observed damage of those case study buildings, conforms to that obtained by Vector-blast analysis. The expected blast damage as well as the level of protection needed for a reinforced concrete structure, can be well predicted for a specific charge weight, way of implementing explosive charge and standoff distance. The study presents tables and figures that would help in predicting the damage level for various charge weights and standoff distances.

References

Dharaneepathy, M.V., Keshava Rao, M.N. and Santhakumar, A.R. 1995. Critical Distance for Blast Resistant Design. *International Journal of Computers and Structures*, **54**(4), pp. 587-595.

FEMA 426, 2003. Reference Manual to Mitigate Potential Terrorist Attacks against Buildings, Risk Management Series, *US department of Homeland Security*, Washington, USA.

Hyde, D.W. 1992. CONWEP, Conventional Weapons Effects Program. U.S. Army Engineer Waterways Experiment Station, Vicksburg, M.S.

Jayasooriya, R. 2010. Vulnerability and Damage analysis of reinforced concrete framed buildings subjected to near field blast events. Ph.D. thesis, *Faculty of Built Environment and Engineering*, Queensland University of Technology, Brisbane, Australia.

Kakogiannis, D., Van Hemelrijck, D., Wastiels, J. Palanivelu, S., Van Paepegem, W., Vantomme, J. Kotzakolios, A. and V. Kostopoulos. 2010. Assessment of Pressure Waves Generated by Explosive Loading. *Tech Science Press, CMES*, **65**(1), pp.75-92.

Miller, P. 2004. Towards the modeling of blast loads on structures. M.A. Sc. thesis, *Department of Civil Engineering*, University of Toronto, , Canada.

Moon, N.N. 2009. Prediction of blast loading and its impact on buildings. M.T thesis, *National Institute of Technology*, Department of Civil Engineering, Rourkela-769008.

Netherton, M.D. and Stewart, M.G. 2016. Risk-based blast-load modeling: Techniques, models and benefits. *International Journal of Protective Structures* 2016, **7**(3), pp. 430–451.

Pranata, Y.A. and Madutujuh, N. 2012. Dynamic time history analysis of blast resistant door using blast load modeled as impact load. *Civil Engineering Forum*. **XXII/1** - January 2012.

Ripley, R.C, von Rosen, B., Ritzel, D.V., and Whitehouse, D.R. 2004. Small-Scale Modeling of Explosive Blasts in Urban Scenarios. *21st International Symposium on Ballistics*, Adelaide, Australia.

Shallan, O., Eraky, A., Sakr, T., and Emad, S. 2014. Response of Building Structures to Blast Effects. *International Journal of Engineering and Innovative Technology (IJEIT)*, **4**(2), ISSN: 2277-3754.

TM 5-1300, Department of the Army. 1990. Structures to resist the effects of accidental explosions. https://en.wikipedia.org/wiki/TNT_equivalent
https://en.wikipedia.org/wiki/Oklahoma_City_bombing
https://en.wikipedia.org/wiki/Khobar_Towers_bombing
https://en.wikipedia.org/wiki/2004_Sinai_bombings
https://en.wikipedia.org/wiki/Islamabad_Marriott_Hotel_bombing
<https://www.christianheadlines.com/news/trauma-grips-survivors-of-church-blast-in-alexandria-egypt-11644990.html>
<https://www.ahram.org.eg/NewsPrint/251330.aspx>
https://en.wikipedia.org/wiki/December_2013_Mansoura_bombing
<http://www.albawabhnews.com/354381>
<https://www.mobtada.com/details/317956>
<https://www.cbsnews.com/news/italian-consulate-bombed-in-cairo-egypt/>
<https://www.hsd1.org/?abstract&did=4506>